

Analysis of Femtocell Coverage Fraction and Isolated Probability Using Stochastic Geometry

Huanle Zhang¹, Jian Liu², Yupeng Jia³, Yulu Ma⁴

¹School of Communication and Information Engineering,

University of Electronic Science and Technology of China (UESTC), Chengdu 611731, China

²University of Science and Technology Beijing (USTB), Beijing 100083, China

³System Engineering America - RF and Communications, National Instruments (NI), Austin, TX, USA

⁴China Telecom Shanghai Research Institute, Shanghai 200122, China

Email: zhanghuanle1342@gmail.com, liujian@ustb.edu.cn, yupeng.jia@ni.com, mayl@sttri.com.cn

Abstract—The deployment of femtocells can effectively improve cellular network capacity without any significant increase in the network management costs. Femtocell base stations are usually installed by users which poses unique challenges for future mobile communication standards. The randomness of the locations of femtocells brings us a lot of difficulties to analyze and compare. In this paper, femtocell coverage fraction and femtocell base station isolated probability are explored with the aid of stochastic geometry. Firstly, we assume that femto base stations are installed randomly following homogeneous Poisson point process and discuss issues about femtocell coverage fraction. It is demonstrated that the coverage fraction closely relates with femtocell coverage radius. We find that in order to effectively cover macro area, the femtocell coverage radius of at least 20 meters should be guaranteed. Corresponding femtocell isolated probability is also explored which is a vital index in realistic issues such as handover. Then, we add restriction on the minimum distance between each femtocell base station and compare the performance of cases with and without restrictions. This paper provides a new prospective on femtocell coverage fraction and isolated probability and the results can be used for femtocell deployment.

I. INTRODUCTION

Femtocell access points (FAPs), also called “home base stations”, are crucial for next generation cellular networks. Femtocells can effectively improve cellular network capacity without any significant increase in the network management costs [1-2]. FAPs are usually installed by users and deployed in indoor environments. These low-power base stations provide a limited coverage area and connect to the operators’ core networks through digital subscriber line (DSL), cable broadband connection, or even wireless links [3].

The interest in femtocells continues to grow in the mobile operator community, and the commercial deployments have increased to 41 in 23 countries during 2012 [4]. It is estimated by Informa Telecoms & Media that the deployments of small cell market would reach 91.9 million by 2016, with femtocells accounting for more than 80%. It is expected FAPs would be

widely deployed in the near future. Though femtocells can offload traffic from the macro stations and are crucial for next generation mobile communications, special challenges exist due to the randomness of the locations of femtocells [5]. Readers can refer to [6-7] for more information about the development of femtocell technology.

Because femtocell base stations are installed by non-expert users, it would present very different characteristics such as the locations of FAPs. The randomness of the locations of femtocells brings us a lot of difficulties to analyze and compare. In order to quantitatively analyze the performance on femtocells, stochastic geometry has been used in some papers. In [8], the authors regard stochastic geometry as one of the four effective tools to solve small cell problems (other three tools are large random matrix theory, Game theory, and interference alignment and VFDM). The authors in [9] propose a tractable approach to solve the problem of SINR distribution for femtocell networks using stochastic geometry while in [10], fractional frequency reuse for OFDMA cellular networks is solved. Those works are based on homogeneous Poisson point process to model the locations of FAPs. One advantage of this approach is the ability to capture the non-uniform layout of modern cellular deployments due to topographic, demographic, or economic reasons [11]. Additionally, tractable expressions can be drawn from the Poisson model, leading to more general performance characterizations and intuition [12].

In this paper, crucial issues such as the femtocell coverage fraction and femtocell isolated probability are explored. The femtocell coverage fraction is a vital index. For instance, how much region will be covered if we use femtocells to offload a certain macrocell region. Because these base stations are deployed randomly, so a very different characteristics would be expected. Besides the femtocell coverage fraction, isolated probability is also considered because it’s important in issues such as handover and cooperative communication. Other than conventional planned deployment, regions of femtocells overlap with each other, so determining isolated probability is a crucial issue since handover to isolated femtocells would be inefficient for users.

The contribution of this paper is solving the problems of the effects of femtocell coverage radius and femtocell density on femtocell coverage fraction and isolated probability in

This work is supported by National Major Projects (No. 2012ZX03001029-005, 2012ZX03001032-003), National Natural Science Foundation of China (Nos. 60932002, 61173149), and Fundamental Research Funds for the Central Universities (No. FRF-TP-12-080A).

femtocell networks, which can be used to aid the design of femto base stations and to guide femtocell deployment. All the results are tractable. As far as we know, no other papers have explored these issues. In this paper, we use homogeneous Poisson point process (p.p.) to quantitatively analyze femtocell coverage fraction and femtocell isolated probability. Then, we add limitation on minimum distance between each femtocell and evaluate the system performance (the corresponding model is Matérn core point process).

This paper is organised as follows: system model is given in Section II which provide preliminaries on homogeneous Poisson point process. Effect of femtocell coverage radius and femtocell density on femtocell coverage fraction and isolated probability with and without restrictions are presented in Section III and Section IV, respectively. Special consideration is given to the femtocell coverage radius of 20 meters to observe how performance changes with femtocell intensity and minimum distance. Finally, Section IV concludes this paper.

II. SYSTEM MODEL

In this section, our system model is explained and relevant assumptions are clarified. This paper is mainly based on two models: homogeneous Poisson point process and Matérn point process. Because Matérn point process can be constructed from Poisson point process (clarified in Section IV), so the main focus of this part is on Poisson point process. The definition of Poisson point process is given below.

Definition 1: Let Λ be a locally finite non-null measure on \mathbb{R}^d . The Poisson point process Φ of intensity measure Λ is defined by means of its finite-dimensional distributions:

$$P\{\Phi(A_1) = n_1, \dots, \Phi(A_k) = n_k\} = \prod_{i=1}^k (e^{-\Lambda(A_i)} \frac{\Lambda(A_i)^{n_i}}{n_i!}), \quad (1)$$

for every $k = 1, 2, \dots$ and all bounded, mutually disjoint sets A_i for $i = 1, \dots, k$. If $\Lambda(dx) = \lambda dx$ is a multiple of Lebesgue measure (volume) in \mathbb{R}^d , then Φ is a homogeneous Poisson point process and λ is the intensity.

The realization of Poisson point process can be constructed as follows. If the region considered has an area of $|A|$, the mean number of points in this region is $\lambda \cdot |A|$. The homogeneous Poisson p.p. can be simply produced by a random variable X following Poisson distribution with parameter $\lambda \cdot |A|$, and each point is distributed uniformly among the region. Fig. 1 shows a snapshot from a homogeneous Poisson point process with intensity equal to $200 / (500 \times 500)$. As shown in Fig. 1, the locations of points seem to be stochastic, but it would resemble the locations of FAPs in the near future.

In this paper, elaborative interaction between macrocell base station and femtocell base station, as well as interaction among FAPs is ignored. In addition, ideal femtocell coverage is assumed, which means the area outside the coverage radius is assumed to be totally unable to access the FAP. The aim of this paper is to explore the effects of different femtocell coverage radii and densities on issues like coverage fraction and isolated probability, so the assumption of ideal coverage radius would not invalid our analysis.

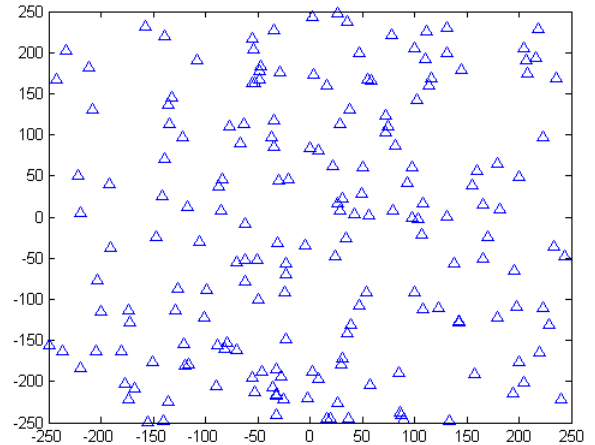


Fig. 1. A snapshot of locations of FAPs taken from a homogeneous Poisson point process with intensity $200 / (500 \times 500)$.

III. COVERAGE FRACTION AND ISOLATED PROBABILITY BASED ON HOMOGENOUS POISSON POINT PROCESS

If we tag each FAP with a mark representing its coverage radius, the corresponding marked Poisson point process is called Boolean Model. In this section, a brief introduction to Boolean model (BM) will be given and how it can be related to femtocell networks is suggested. The Boolean model can be constructed from Poisson point process and is stated below.

Definition 2: Let Φ be a Poisson point process of intensity Λ on \mathbb{R}^d and let marks Ξ_i be some independent and i.i.d sequence which are random closed sets (RACs) of \mathbb{R}^d . Then the associated *Boolean model* is the union:

$$\Xi_{BM} = \bigcup_i (x_i + \Xi_i) \quad (2)$$

In Boolean model, points and RACs are also called germs and grains, respectively. In this paper, we simply regard the points as femtocell base stations and Ξ_i as the coverage range of the i^{th} femtocell. Hence, the Boolean model can be used as a mathematical tool to aid our discussion and analysis.

A. Coverage Volume Fraction

An essential question is what the proportion of area is covered by femtocells given the intensity λ_{femto} . *Theorem 1* can be used to answer the question.

Theorem 1: The homogeneous Boolean model with intensity λ and generic grain Ξ has the volume fraction

$$p = 1 - e^{-\lambda \mathbb{E}[|\Xi|]}. \quad (3)$$

Proof: let $\tilde{\Phi}$ be a marked Poisson p.p. generating the BM as in *Definition 2*. For a given compact K define the point process

$$\Phi_K = \sum_{(x_i + \Xi_i) \cap K \neq \emptyset} \varepsilon_{x_i} \mathbb{1}((x_i + \Xi_i) \cap K \neq \emptyset).$$

This is an independent thinning of the points of $\tilde{\Phi}$ with the thinning probability

$$p_K(x) = P\{(x + \Xi) \cap K \neq \emptyset\} = P\{x \in \check{\Xi} \oplus K\}.$$

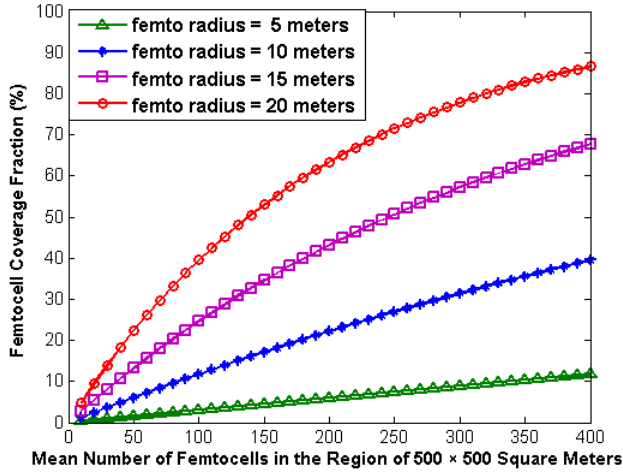


Fig. 2. Femtocell coverage fraction in a region of 500×500 square meters. Four scenarios are drawn: femtocell radius equals 5, 10, 15 and 20 meters, respectively. The intensity is equal to the mean number of femtocells divided by the area.

Obviously, Φ_K is a Poisson p.p. with intensity measure $p_k(x)\Lambda(dx)$. By Fubini's theorem,

$$\begin{aligned} \int_{\mathbb{R}^d} p_K(x)\Lambda(dx) &= \int_{\mathbb{R}^d} P\{x \in \Xi \oplus K\} \\ &= \mathbb{E}[\int_{\mathbb{R}^d} \mathbb{1}((x_i + \Xi_i) \cap K \neq \emptyset)] = \mathbb{E}[\Lambda(\Xi \oplus K)]. \end{aligned}$$

Hence, the number of grains of the BM intersecting a given compact K is a Poisson random variable N_K with parameter $\mathbb{E}[\Lambda(\Xi \oplus K)]$. Due to the translation invariance of the RAC, the volume fraction can also be expressed as the probability that a given point (say the origin) is covered by Ξ . Indeed,

$$\begin{aligned} p &= \frac{\mathbb{E}[|\Xi \cap B|]}{|B|} = \frac{1}{|B|} \int E[\mathbb{1}(x \in \Xi)]dx = P\{0 \in \Xi\} \\ &= P\{\Xi \cap \{0\} \neq \emptyset\} = 1 - e^{-\mathbb{E}[\Lambda(\Xi \oplus \{0\})]} = 1 - e^{-\lambda \mathbb{E}[|\Xi|]}. \end{aligned}$$

Fig. 2 shows how the volume fraction changes as the mean number of femtocell base stations increases under the conditions of different femtocell coverage scenarios (each scenario considers constant FAP coverage radius) in a region of 500×500 square meters. Take the scenario of the radius of 20 meters for example, if the femtocells are employed in a planned way, the number of femtocells needed is $500 \times 500 / (\pi \cdot 20^2) \approx 199$ to cover the whole macrocell region. However, if the femtocell base stations are employed by users, it can be seen from Fig. 2 that 400 femtocells cannot occupy 90% of the region. With the lower radius, a remarkable less coverage fraction can be seen. From Fig. 2, we can get following information:

- If the coverage radius of each FAP is below 10 meters, then even in the dense deployment situation, these femtocells cannot cover the whole region if they are installed randomly. It's obvious from Fig. 2 that if the radius equals to 5 meters, on average, 400 femtocell base stations can only cover about 10% of the region of 500×500 square meters, which is contradictory to our intuition.
- If we want to use femtocells to assist covering the macro region, then the femtocell radius should not be too small. At least 15 meters should be guaranteed.

Larger than 20 meters is ideal if we want to offload macro traffic effectively.

- If we want to use femtocells to cover a large portion of macro areas, it is advised not to install these femtocell base stations completely randomly. Some restrictions should be imposed on the locations of femtocell base stations.

B. Isolated Probability

Due to the randomness property of femtocell deployment, there would be femtocell areas that are overlapping with each other (which can be inferred from Fig. 1). In order to reduce interference and frequent handover, these overlapping femtocells should be clustered and coordinated. In this case, the interference will be alleviated and overheads of handovers between femtocells are negligible compared to uncoordinated femtocells. By directly interacting between overlapping femtocells or by femtocell gateway, the preceding assumption is reasonable. There are also isolated femtocells that are disjointed from other femtocells. Special consideration should be given to these isolated femtocells to avoid frequent handover, which definitely results in degraded user experience. Thus, a realistic question is what the probability that femtocells are isolated. *Theorem 2* can be used to answer this question.

Theorem 2: Consider homogeneous BM Ξ_{BM} in \mathbb{R}^d with intensity λ . Let variable R denote the radius of the circle coverage of the grains. Assume that $E[R^d] < \infty$. Then, the probability that a typical grain of radius R_0 is isolated is equal to

$$P\{B_0(R_0) \cap \Xi_{BM} = \emptyset\} = E[e^{-\lambda v_d \sum_{k=0}^d \binom{d}{k} R_0^{d-k} E[R^k]}], \quad (4)$$

and v_d is the volume of a unit-radius ball in \mathbb{R}^d .

Proof: conditioning on the radius $R_0 = r$ of typical grain $B_0(R_0)$ located at the origin under P , all other points whose grains are not disjoint from $B_0(r)$ form an independent thinning of the marked p.p. $\tilde{\Phi}' = \sum_{i:|x_i| \neq 0} \mathcal{E}_{(x_i, B_0(R_i))}$. The retention probability for x_i with radius R_i is $p_r(x_i, R_i) = P\{r + R_i \geq |x_i|\}$. By Slivnyak's theorem, the thinning is a non-homogeneous Poisson p.p. with intensity measure Λ such that

$$\begin{aligned} \Lambda(\mathbb{R}^d) &= \lambda \int_{\mathbb{R}^d} \int_{\mathbb{R}^+} p_r(x, s) ds F(ds) \\ &= \lambda v_d \sum_{k=0}^d \binom{d}{k} r^{d-k} E[R^k] := \gamma(r), \end{aligned}$$

where F is the distribution of R . Consequently, the probability that $B_0(r)$ is isolated is equal to $e^{-\gamma(r)}$ and equation (4) follows when de-conditioning with respect to the radius $R_0 = r$. ■

In this paper, we only consider 2-dimensional space and fixed femtocell coverage radius in each scenario, so the isolated probability for scenarios with the radius of R can be reduced to:

$$P\{\text{femto coverage radius of } R\} = e^{-4 \cdot \pi \cdot \lambda \cdot R^2} \quad (5)$$

Fig. 3 shows the corresponding isolated probability for different femtocell coverage radii. From this figure, we can get the following information:

- It's certain that in each scenario, when the density of femtocells is small, femtocells tend to be isolated.

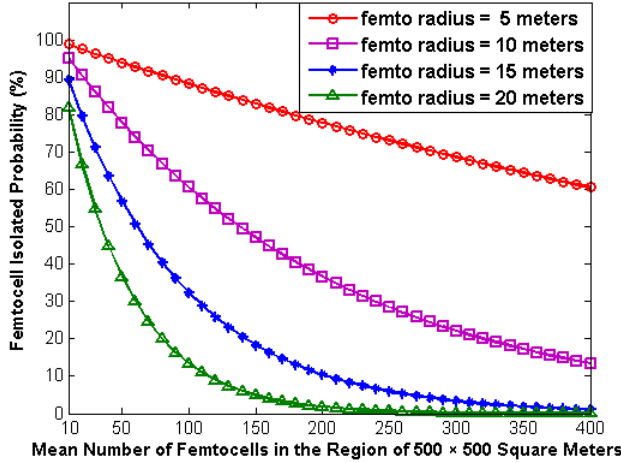


Fig. 3. The femtocell isolated probability for different coverage radii in a region of 500×500 square meters. Four scenarios are drawn: femtocell radius equals 5 meters, 10 meters, 15 meters and 20 meters, respectively.

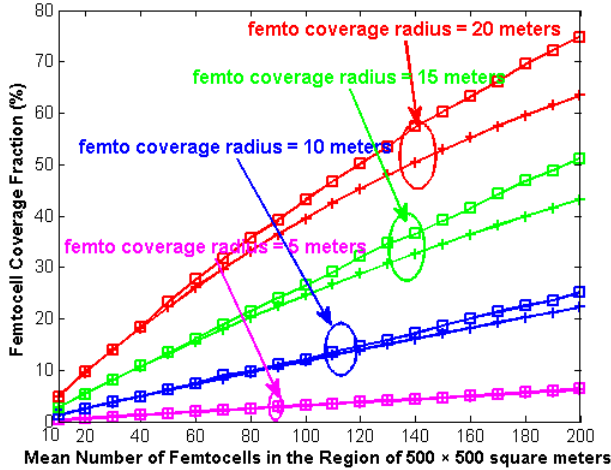


Fig. 4. The femtocell coverage fraction in a region of $500 \times 500m$. Four scenarios are drawn: femtocell radius equals 20m, 15m, 10m, and 5m, respectively. The lines with square markers belong to the Matérn hard core model, whereas the lines with '+' markers belong to the corresponding homogeneous Poisson point process.

As the density of femtocells increases, the isolated probability decreases in an exponential rate.

- If the femtocell base stations that are used to offload traffic from macro base stations have a constant radius less than 10 meters, most of femtocells would be isolated. In this situation, clustering multiple femtocells into “one” femtocell would be inefficient. Consequently, special considerations should be taken to combat the handover question in those cases.
- If we want to offload traffic from macro base stations and to use the method of clustering multiple femtocells to form a large and coordinative femtocell to alleviate interference and handover issues, the preferable radius for each femtocell should be larger than 20 meters.

IV. COVERAGE FRACTION AND ISOLATED PROBABILITY BASED ON MATÉRN CORE POINT PROCESS

From preceding analysis, the coverage fraction is unsatisfactory in the case of homogeneous Poisson point process (i.e., femto base stations are installed by users and no restrictions are forced). A natural consideration is how the coverage fraction and isolated probability change if we put limitation on the minimum distance between femtocell base stations. The corresponding model is the Matérn core Point Process, or Matérn Hard Core (MHC) model as well.

The Matérn hard core point process can be constructed from an underlying Poisson p.p. by removing certain points depending on the positions of the neighboring points and additional marks attached to the points. The construction procedure of the Matérn hard core point process is outlined as follows.

Let Φ be a Poisson p.p. with intensity λ on \mathbb{R}^d : $\Phi = \sum_i \varepsilon_{x_i}$ and h be the minimum distance between each femtocell base stations. Considering the following independently marked version of this process: $\tilde{\Phi} = \sum_i \varepsilon_{(x_i, U_i)}$, where U_i are random variables uniformly distributed on $[0, 1]$. Define new marks m_i of points of $\tilde{\Phi}$ by $m_i = 1(U_i < U_j \text{ for all } y_j \in B_{x_i}(h) \setminus \{x_i\})$. Interpreting U_i as the “age” of point x_i , one can say that m_i is the indicator that the point x_i is the “youngest” one among all the points in its neighborhood $B_{x_i}(h)$. The Matérn hard core point process is defined by: $\Phi_{MHC} = \sum_i m_i \varepsilon_{x_i}$. Φ_{MHC} is an example of a dependent thinning of $\tilde{\Phi}$, however, the resulting MHC p.p. is not a Poisson p.p..

In order to compare the difference of the coverage fraction with restriction on the minimum distance, the intensity or the mean number of femtocell base stations must be equal with their homogeneous Poisson point process counterpart. In this paper, we only consider 2-dimensional space and the corresponding intensity of the Matérn hard core model λ_{MHC} is:

$$\lambda_{MHC} = \frac{1 - e^{-\lambda \cdot \pi h^2}}{\pi h^2}, \quad (6)$$

where h is the minimum distance between each femto base stations and λ is the intensity of the underlying homogeneous Poisson point process.

Proof: first, we identify the distribution of marks by finding the distribution of the typical mark of $\tilde{\Phi}_{MHC}$ and then calculating the intensity λ_{MHC} of the p.p. $\tilde{\Phi}_{MHC}$. For $B \subset \mathbb{R}^d$ and $0 \leq a \leq 1$, according to Slivnyak’s theorem,

$$\begin{aligned} & \tilde{C}(B \times ([0, a] \times \{1\})) \\ &= \mathbb{E}[\int_B \int_{[0, a]} \mathbb{1}(u < U_j \text{ for all } y_j \in B_x(h) \cap \Phi \setminus \{x\}) \tilde{\Phi}(d(x, u))] \\ &= \lambda |B| \int_B \int_0^a P\left\{\sum_{(x_j, U_j) \in \tilde{\Phi}} \mathbb{1}(U_j \leq u) \varepsilon_{x_j}(B_x(h)) = 0\right\} dudx \\ &= \lambda |B| \int_0^a e^{-\lambda \pi u h^2} du = |B| \cdot \frac{1 - e^{-\lambda \pi h^2}}{\pi h^2}. \end{aligned}$$

In order to calculate the intensity λ_{MHC} of the Matérn p.p., we take a set B with $|B| = 1$ and obtain

$$\lambda_{MHC} = \tilde{C}(B \times ([0, 1] \times \{1\})) = \frac{1 - e^{-\lambda \pi h^2}}{\pi h^2},$$

which concludes the proof. \blacksquare

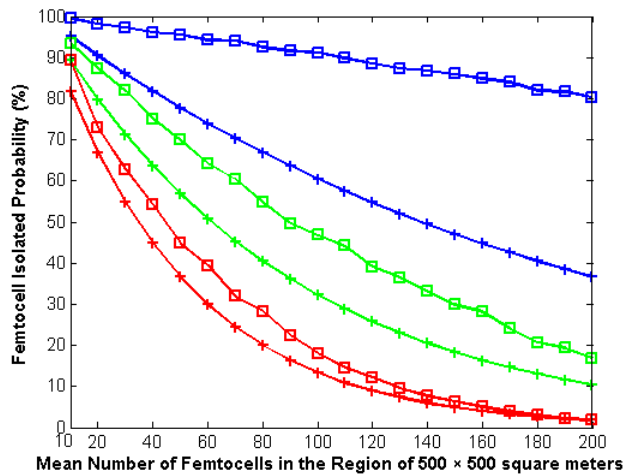


Fig. 5. The femtocell isolated probability for both models: homogeneous Poisson point process and the Matérn hard core(MHC) point process. The lines with square markers belong to the Matérn hard core point process, while the lines with '+' markers belong to the homogeneous Poisson point process. The blue, green and red lines present the scenarios of femtocell coverage radius of 10 meters, 15 meters and 20 meters, respectively.

Certainly, the intensity must be positive and the limite value for λ_{MHC} is $\frac{1}{v_d h^d}$, when $\lambda \rightarrow \infty$. In the region of 500×500 square meters, if the minimum distance $h = 18$ meters, then the maximal mean number of FAPs in Matérn hard core model is just over 200. In the following part, simulation is used to determine its femtocell coverage fraction and isolated probability.

A. Coverage Volume Fraction

Throughout this paper, we mainly focus on the femtocell coverage radii of 5 meters, 10 meters, 15 meters and 20 meters. In comparison, the intensities of Matérn hard core model and homogeneous Poisson point process are equated and we assume that the minimum distance h is 18 meters in this part and observe how performance changes.

Fig. 4 shows the femtocell coverage fraction in the region of 500×500 square meters. From this figure, we achieve the following information:

- For the cases where each femtocell's coverage radius is small (e.g., 5 meters and 10 meters), even if we add minimum distance restriction as high as 18 meters, the improvements of the coverage fraction are not noticeable. Even when the mean number of femtocells in the region considered reaches 200, we can only see 0.3% and 3.2% improvements in the case of 5 meters and 10 meters, respectively. Consequently, in the cases of small coverage radii, adding restrictions on minimum distance is not an effective method.
- The improvement of the coverage fraction is more appreciable with the coverage radius increasing. In the case of 20 meters, the improvement is 11.2% when the mean number of femtocells is 200, which occupies the area from 63.4% to 75.6%. As shown in Fig. 2, it needs about 290 femtocell base stations to cover the 75.6% area in the case of no restrictions, saving

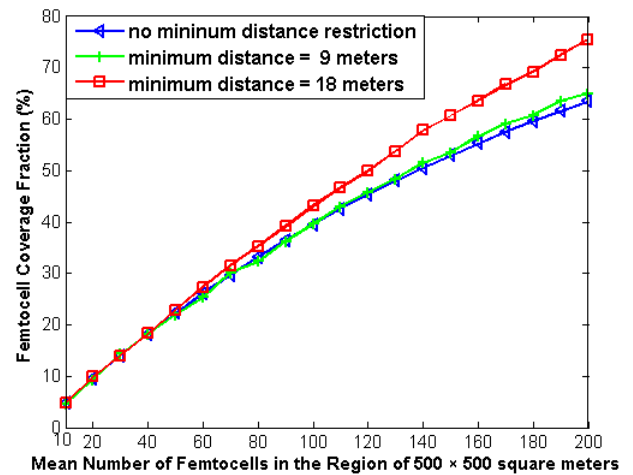


Fig. 6. The femtocell coverage fraction. Red line represents the case when the minimum distance is 18 meters while the green line represents the 9 meters case. The femtocell coverage radius is 20 meters

about $(290 - 200)/290 \times 100\% \approx 31\%$ of femtocell base stations

B. Isolated Probability

We have seen that the improvement of the coverage fraction is noticeable when the femtocell coverage radius isn't too small (at least 10 meters should be guaranteed). In this part, the femtocell isolated probability will be explored. Because minimum distance of $h = 18$ meters is assumed here, so we omit the situation when the coverage radius is 5 meters in that those femtocells never "touch" each other. The femtocell isolated probabilities based on both models are depicted in Fig. 5.

It can be seen from Fig. 5 that the difference of the femtocell isolated probability increases at first and then decreases until there is no difference when the deployment is dense. In all three scenarios, the isolated probabilities are larger than their counterparts. However, the difference is lower in the scenario of larger femtocell coverage radius (see the scenario of femtocell coverage radius of 20 meters).

Femtocell radius of 20 meters would be a best candidate if we combine its femtocell coverage fraction, isolated probability and realistic factors into consideration. In the following subsection, we will explore specially the scenario of 20 meters as we put different minimum distances to observe how the coverage fraction and isolated probability change.

C. Special Consideration on Femtocell radius of 20 meters

Considering the femtocell coverage fraction, isolated probability and realistic factors, femtocell radius of 20 meters would be the best choice. Hence, in this subsection, we will explore how the minimum distance affects the overall performance.

Fig. 6 shows the femtocell coverage fraction when the minimum distance is 18 meters and 9 meters respectively, which are compared with the case when no minimum distance is restricted. It can be seen from the figure that adding a small

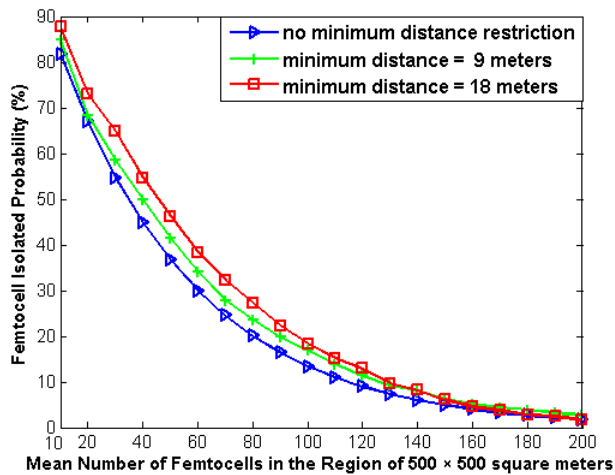


Fig. 7. The femtocell isolated probability. Red line represents the scenario when the minimum distance is 18 meters while the green line represents the 9 meters case. The femtocell coverage radius is 20 meters

minimum distance cannot improve the total femtocell coverage fraction very much. Specifically, even the minimum distance is 9 meters, no appreciable improvement can be noticed. However, limiting the minimum distance to 18 meters dose improve the femtocell coverage fraction obviously. It can be concluded from Fig. 6 that if we want to improve the femtocell coverage fraction through adding minimum distance limitation, a certain distance should at least be guaranteed; otherwise, the effect is in vain (in the 20 meters case, minimum distance less than 10 meters is ineffective).

Fig. 7 shows the femtocell isolated probability when the minimum distance is 9 meters and 18 meters respectively, and compared with the case when no minimum distance is restricted. It can be seen from the figure that both restricted cases display noticeable difference when the femtocell deployment is slightly dense. However, as the femtocell density increases, the difference decreases. We can also see that when the mean number of femtocell is 160, the isolated probability for the minimum distance of 18 meters case is 4.6% while in the no restriction case is 4.0%. Thus, the difference is only 0.6%. However, the coverage fraction is 63.6% in the case of 18 meters and 55.3% in the case of no restriction (which can be seen from Fig. 6), so a 8.3% difference can be noticed. An interesting phenomenon can be witnessed from the figure that the case of minimum distance of 18 meters is converged more rapidly to the no restriction case than its counterpart 9 meters as the femtocell density increases. As the femtocell deployment density increase, a less difference of the isolated probabilities and a higher difference of coverage fraction can be seen. Consequently, in the case of 20 meters coverage radius, minimum distance of 18 meters is much preferred to the 9 meters case and no restriction case when the mean number of FAPs is higher than 160 in a region of 500×500 square meters.

V. CONCLUSION

Because femtocell base stations are installed by non-expert users, it would present much different characteristics such as the locations of femtocells. The randomness of the locations

of femtocells brings us a lot of difficulties to analyze and compare. In this paper, we used stochastic geometry to quantitatively analyze the effect of different femtocell coverage radii and femtocell densities on issues such as femtocell coverage fraction and isolated probability.

Firstly, Boolean model is used in this paper to analyze the femtocell coverage fraction and isolated probability, assume that the femtocell base stations are equally located at macro region considered. Then, we add restriction on minimum distance between each femtocell base stations and corresponding performances are analyzed and compared with the preceding cases. From exhaustive analysis about the femtocell coverage fraction, isolated probability and realistic factors, the femtocell coverage radius of 20 meters is most ideal and special consideration is given to this case. The paper gives a new perspective on the femtocell issues such as the coverage fraction and isolated probability.

REFERENCES

- [1] V. Chandrasekhar, J. G. Andrews, and A. Gatherer, "Femtocell Networks: A Survey," *IEEE Commun. Mag.*, vol. 46, no. 9, pp. 59-67, Sept. 2008.
- [2] H. Claussen, L. T. W. Ho, and L. G. Samuel, "Financial Analysis of a Pico-Cellular Home Network Deployment," *IEEE Intern. Conf. on Commun. (ICC)*, pp. 5604-5609, June 2007.
- [3] H. Claussen, "Performance of Macro- and Co-Channel Femtocells in a Hierarchical Cell Structure", *IEEE 18th Symp. on Personal, Indoor and Mobile Radio Comm. (PIMRC)*, pp. 1-5, Sept. 2007.
- [4] Small Cell Forum, <http://www.smallcellforum.org>, 2012.
- [5] J. G. Andrews, H. Claussen, M. Dohler, S. Rangan, and M. C. Reed, "Femtocells: Past, Present, and Future," *IEEE Journal on Selected Areas In Communications*, vol. 30, no. 3, April 2012.
- [6] Shanzhi CHEN, Yingmin WANG, Weiguo MA, and Jun CHEN, "Technical Innovations Promoting Standard Evolution: From TD-SCDMA to TD-LTE and Beyond," *IEEE Wireless Communications*, Vol. 19, no. 2, pp. 60-66, Feb. 2012.
- [7] Long Yu, Jian Liu, and Keping Long, "Analysis of Virtual MIMO-based Cooperative Communication in Femtocell Network," *IEEE Globecom 2011*, Houston, TX, USA, pp: 1-5, Dec. 2011.
- [8] J. Hoydis, and M. Debbah, "Green, Cost-effective, Flexible, Small Cell Networks," *IEEE Comm. Soc. MMTC*, vol. 5, no. 5, pp. 23-26, Oct. 2010.
- [9] J. G. Andrews, F. Baccelli, and R. K. Ganti, "A Tractable Approach to Coverage and Rate in Cellular Networks," *IEEE Transactions on Communications*, vol. 59, no. 11, November 2011.
- [10] T. D. Novlan, R. K. Ganti, A. Ghosh, and J. G. Andrews, "Analytical Evaluation of Fractional Frequency Reuse for OFDMA Cellular Networks," *IEEE Transactions on Communications*, vol. 10, no. 12, December 2011.
- [11] M. Haenggi, J. Andrews, F. Baccelli, O. Dousse, and M. Franceschetti, "Stochastic geometry and random graphs for analysis and design of wireless networks," *IEEE J. Sel. Areas Commun.*, vol. 27, no. 7, pp. 1029-1046, Sep. 2009.
- [12] R. K. Ganti, F. Baccelli, and J. G. Andrews, "A new way of computing rate in cellular networks," in *Proc. IEEE International Conference on Communicaitons*, June 2011.